




# Quantification and Proximal-to-Distal Distribution Pattern of Tibial Nerve Lesions in Relapsing-Remitting Multiple Sclerosis

## Assessment by MR Neurography

Adriana M. Pietsch<sup>1,2</sup> · Andrea Viehöver<sup>3</sup> · Ricarda Diem<sup>3</sup> · Markus Weiler<sup>3</sup> · Mirjam Korporal-Kuhnke<sup>3</sup> · Brigitte Wildemann<sup>3</sup> · Georges Sam<sup>3</sup> · John M. Hayes<sup>4</sup> · Olivia Fösleitner<sup>1</sup> · Johann M. E. Jende<sup>1</sup> · Sabine Heiland<sup>5</sup> · Martin Bendszus<sup>1</sup> · Jennifer C. Hayes<sup>1</sup> 

Received: 17 March 2022 / Accepted: 14 September 2022 / Published online: 20 October 2022  
© The Author(s) 2022

### Abstract

**Purpose** Recent studies suggest an involvement of the peripheral nervous system (PNS) in multiple sclerosis (MS). Here, we characterize the proximal-to-distal distribution pattern of peripheral nerve lesions in relapsing-remitting MS (RRMS) by quantitative magnetic resonance neurography (MRN).

**Methods** A total of 35 patients with RRMS were prospectively included and underwent detailed neurologic and electrophysiologic examinations. Additionally, 30 age- and sex-matched healthy controls were recruited. 3T MRN with anatomical coverage from the proximal thigh down to the tibiotalar joint was conducted using dual-echo 2-dimensional relaxometry sequences with spectral fat saturation. Quantification of PNS involvement was performed by evaluating microstructural (proton spin density ( $\rho$ ), T2-relaxation time ( $T2_{app}$ )), and morphometric (cross-sectional area, CSA) MRN markers in every axial slice.

**Results** In patients with RRMS, tibial nerve lesions at the thigh and the lower leg were characterized by a decrease in  $T2_{app}$  and an increase in  $\rho$  compared to controls ( $T2_{app}$  thigh:  $p < 0.0001$ ,  $T2_{app}$  lower leg:  $p = 0.0040$ ;  $\rho$  thigh:  $p < 0.0001$ ;  $\rho$  lower leg:  $p = 0.0098$ ). An additional increase in nerve CSA was only detectable at the thigh, while the semi-quantitative marker T2w-signal was not altered in RRMS in both locations. A slight proximal-to-distal gradient was observed for  $T2_{app}$  and T2-signal, but not for  $\rho$ .

**Conclusion** PNS involvement in RRMS is characterized by a decrease in  $T2_{app}$  and an increase in  $\rho$ , occurring with proximal predominance at the thigh and the lower leg. Our results indicate microstructural alterations in the extracellular matrix of peripheral nerves in RRMS and may contribute to a better understanding of the pathophysiologic relevance of PNS involvement.

**Keywords** Magnetic resonance neurography · Peripheral nervous system · Quantitative imaging markers · Proton spin density · T2-relaxometry

✉ Jennifer C. Hayes  
jennifer.hayes@med.uni-heidelberg.de

<sup>1</sup> Department of Neuroradiology, Heidelberg University Hospital, Im Neuenheimer Feld 400, 69120 Heidelberg, Germany

<sup>2</sup> Department of Internal Medicine, Spital Walenstadt, Walenstadt, Switzerland

<sup>3</sup> Department of Neurology, Heidelberg University Hospital, Heidelberg, Germany

<sup>4</sup> Department of Neurology, University of Michigan, Ann Arbor, USA

<sup>5</sup> Division of Experimental Radiology, Department of Neuroradiology, Heidelberg University Hospital, Heidelberg, Germany

## Introduction

Multiple sclerosis (MS) is traditionally regarded as an autoimmune chronic inflammatory demyelinating disease restricted to the central nervous system (CNS). The exact etiology and pathomechanism remains unclear, but a multifactorial genesis combining genetic and environmental factors, such as low vitamin D levels, is currently favored [1]. Initial clinical manifestations often affect patients' vision due to optic neuritis or lead to sensory or motor impairments [2, 3]. Later on, further motor restrictions, autonomic dysfunction [4] and neuropsychologic symptoms can occur [5, 6]. Approximately 90% of all cases manifest as relapsing-remitting MS (RRMS), with some cases transforming into secondary progressive MS (SPMS), while the remaining 10% are considered as chronic progressive (CPMS) [7, 8]. With the latest revision of the McDonald criteria from 2017, the diagnosis of MS can be established after one single clinical event when magnetic resonance imaging (MRI) of the CNS confirms a dissemination of inflammatory lesions in space and time [9].

An involvement of the peripheral nervous system (PNS) in MS has been controversially discussed in the literature since early histopathologic studies found areas of demyelination in peripheral nerves of deceased MS patients [10–12]. Electrophysiologic studies were published with inconclusive findings neither proving nor refuting a PNS involvement [13, 14]. In a recent proof-of-concept study applying high-resolution MR neurography (MRN), PNS lesions in the sciatic nerves of MS patients were for the first time visualized in vivo [15]. In that study, nerve abnormalities were derived from alterations of the T2w signal, [15] a per se unspecific marker that cannot be directly quantified, and that might be influenced by external factors such as field inhomogeneities, or different signal attenuation for the imaged slabs [16]. However, additional nerve lesion quantification, using T2-relaxometry, was only performed at a small anatomical region at the distal thigh.

With this study, we aimed to characterize and quantify PNS involvement on a microstructural level by applying T2-relaxometry, and to identify the proximal-to-distal nerve lesion distribution pattern in a clinically and electrophysiologically well-characterized cohort of patients with RRMS in comparison with healthy controls.

## Methods

### Study Design

This cross-sectional, single center study was approved by the local ethics committee (S-405/2012) and all participants gave written informed consent according to the

Declaration of Helsinki. Overall, 35 patients with RRMS (12 males, 23 females, mean age  $37.7 \pm 2.2$  years, range 20–64 years, 2017 McDonald criteria fulfilled in all patients) were prospectively enrolled between January 2017 and December 2019. Additionally, 30 sex-matched and age-matched healthy volunteers (14 males, 16 females, mean age  $36.8 \pm 2.3$  years, range 19–64 years) were recruited. Exclusion criteria were age < 18 years, pregnancy, any contraindications for MRI, any risk factors for neuropathy such as alcoholism, diabetes, malignant or infectious diseases, a transition to secondary progressive multiple sclerosis, any therapy with steroids in the 8 weeks immediately prior to the MRN scans, and any previous exposure to neurotoxic drugs. By taking a detailed past medical history, any sensory or motor symptoms in the upper or lower extremities, any history of neuropathy, any previous spine surgery, and any chronic or malignant diseases were ruled out in all healthy volunteers.

### Clinical and Electrophysiological Examination

A past medical history was taken in all patients and all current and previous disease-modifying pharmacologic therapies were documented. Detailed clinical examination included scoring for the Expanded Disability Status Scale (EDSS) (R.D., A.V., M.K.-K., B.W.). Motor nerve conduction studies (NCS) assessed distal motor latencies (DML), compound muscle action potentials (CMAP), nerve conduction velocities (NCV), and F-waves of the left tibial and peroneal nerves. Sensory nerve action potentials (SNAP) and NCVs were measured for the left sural nerve (M.W., G.S.). Skin temperature was controlled at a minimum of 32°.

### MRN Protocol

All participants underwent high-resolution MRN in a 3T MR-scanner (Magnetom PRISMA, Siemens Healthineers, Erlangen, Germany) by using a 15-channel transmit-receive extremity coil (INVIVO, Gainesville, FL, USA) and the following sequence for T2-relaxometry:

Axial 2D dual echo turbo-spin-echo sequence with spectral fat saturation with four continuous imaging slabs at the left leg. Slab 1: proximal to mid-thigh; slab 2: mid to distal thigh with alignment of the distal edge with the tibiofemoral joint space; slab 3: proximal to mid lower leg with alignment of the proximal edge with the tibiofemoral joint space; slab 4: mid to distal lower leg with alignment of the distal edge with the tibiotalar joint space. One additional slab (slab 5) was acquired at the right leg covering the mid to distal thigh (equal position as slab 2 on the left side). Sequence parameters were: repetition time 5860 ms,

short echo time ( $TE_1$ ) 14 ms, long TE ( $TE_2$ ) 86 ms, field of view  $170 \times 170 \text{ mm}^2$ , matrix size  $512 \times 512$ , slice thickness 3.5 mm, interslice gap 0.35 mm, voxel size  $0.3 \times 0.3 \times 3.5 \text{ mm}^3$ , flip angle  $180^\circ$ , 35 slices, acquisition time per slab 8:25 min.

The net acquisition time for this protocol including survey scans was 44:39 min. Patient and coil repositioning required additional time, resulting in a total examination time of approximately 60 min per participant.

### Image Postprocessing and Statistical Analysis

All MRN images were pseudonymized, and subsequently analyzed with FSL software [17]. The tibial fascicles within the left sciatic nerve and their subsequent continuation as tibial nerve were manually segmented on a total of 140 axial imaging slices per participant from the proximal thigh to the tibiotalar joint space (imaging slabs 1–4) by one investigator blinded to clinical data (A.P.). The epineurium served as an easily visible segmentation border. To exclude relevant side differences, additional segmentation of the tibial fascicles within the right sciatic nerve was performed on 35 axial slices from right mid to distal thigh level (imaging slab 5). This anatomical level was chosen for side comparisons, as previous MRN studies in different polyneuropathies (PNP) as well as preliminary analyses in RRMS detected nerve lesions predominantly in this region [18–21].

### Quantitative and Semiquantitative Signal-based and Signal-independent Analyses

Signal quantification was performed by calculating the microstructural MRN markers,  $T2_{\text{app}}$  and  $\rho$ , according to the two following formulas by using data from the dual echo relaxometry sequence with  $TE_1$  set at 14 ms and  $TE_2$  set at 86 ms. This sequence has been shown to provide equally robust and reliable T2-relaxometry data when calculating  $T2_{\text{app}}$  and  $\rho$  as gold standard multi-echo sequences [22].

$$T2_{\text{app}} = \frac{TE_2 - TE_1}{\ln(SI(TE_1)/SI(TE_2))}$$

$$\rho = \frac{SI(TE_1)}{\exp(-TE_1/T2_{\text{app}})}$$

Mean values of tibial nerve  $T2_{\text{app}}$  and  $\rho$  were calculated per slice position and participant. We refrained from calculating  $\rho$  and  $T2_{\text{app}}$  on a pixel-by-pixel basis, as the high spatial resolution mandatory for MRN results in higher noise levels, which in turn lead to low accuracies of  $\rho$  and  $T2_{\text{app}}$  within single pixels. To decrease the influence of noise, we calculated  $\rho$  and  $T2_{\text{app}}$  from signal intensities determined in the nerve on each slice (region of interest approach).

Averaged mean values of tibial nerve  $T2_{\text{app}}$  and  $\rho$  were then compared between RRMS and healthy controls, as well as between proximal (thigh; imaging slabs 1 and 2) and distal (lower leg; imaging slabs 3 and 4) segments of the tibial nerve along the left leg in order to determine the exact spatial distribution pattern of peripheral nerve lesions in RRMS. Additionally, mean values of tibial nerve  $T2_{\text{app}}$  and  $\rho$  were compared between the left and right mid to distal thigh.

In the same way, mean values for semiquantitative tibial nerve T2w signal were additionally calculated.

Nerve cross-sectional area (CSA) represents a signal-independent, pure morphometric, quantitative MRN marker. Mean CSA of the tibial nerve was recorded per slice position and participant analog to the methods described for signal-based analyses.

### Statistical Analysis

Statistical data analyses were performed with GraphPad Prism version 9.0.2 for Windows (GraphPad Software, San Diego, CA, USA; J.C.H.). The Mann-Whitney test was used to detect differences between (i) RRMS patients and controls, (ii) proximal and distal anatomical locations, and (iii) the right and left leg for all evaluated MRN parameters. Pearson's correlation coefficients were calculated for further correlation analyses between MRN parameters and demographic (participant age, sex, height, weight, body mass index, BMI), clinical (EDSS, duration of symptoms) and electrophysiologic (tibial and peroneal NCV, DML, and CMAP, sural nerve NCV and SNAP) results. Statistical tests were two-tailed and an alpha level of significance was defined at  $p < 0.05$ . All results are documented as mean values  $\pm$  standard error of the mean (SEM).

## Results

### Clinical and Electrophysiologic Data

All 35 RRMS patients fulfilled the revised 2017 McDonald criteria, [9] and with the exception of one therapy-naïve patient, all patients were treated with different disease-modifying drugs. Current or previous disease-modifying drugs included in alphabetic order: alemtuzumab, dimethyl fumarate, fingolimod, glatiramer acetate, interferon beta 1a and 1b, natalizumab, and teriflunomide. Duration of symptoms at the time of MRN acquisition was between 5 months and 27.3 years with 10 of 35 patients being diagnosed within the last 3 years. Besides minor unspecific abnormalities in 12 RRMS patients, electrophysiologic examination results were all in physiologic ranges excluding the presence of a (poly)neuropathy. There were no group differ-

**Table 1** Demographic, clinical, and electrophysiologic data

Parameter	RRMS patients	Controls	P value
Age (years)	37.7±2.2	36.8±2.3	0.72
Sex (M/F)	12/23	14/16	N/A
Body weight (kg)	75.7±2.8	75.1±2.4	0.57
Height (cm)	173.8±1.7	174.3±1.6	0.85
Duration of symptoms (months)	97.6±15.3	N/A	N/A
EDSS (0–10 points)	1.6±0.3	N/A	N/A
Tibial nerve CMAP (mV)	21.3±1.3	N/A	N/A
Tibial nerve NCV (m/s)	50.5±0.9	N/A	N/A
Tibial nerve F-wave (ms)	49.4±1.2	N/A	N/A
Tibial nerve DML (ms)	3.5±0.1	N/A	N/A
Peroneal nerve CMAP (mV)	7.6±0.6	N/A	N/A
Peroneal nerve NCV (m/s)	49.2±1.0	N/A	N/A
Peroneal nerve F-wave (ms)	47.8±1.1	N/A	N/A
Peroneal nerve DML (ms)	4.0±0.1	N/A	N/A
Sural nerve SNAP (μV)	15.2±1.6	N/A	N/A
Sural nerve NCV (m/s)	52.3±1.7	N/A	N/A

Results are presented as mean values ± SEM

CMAP compound muscle action potential, DML distal motor latency, EDSS Expanded Disability Status Scale, N/A not applicable, NCV nerve conduction velocity, RRMS relapsing-remitting multiple sclerosis, SNAP sensory nerve action potential

ences between RRMS patients and healthy controls in terms of age, weight, and height (Table 1). Detailed demographic, clinical, and electrophysiologic data are summarized in Table 1.

## Quantitative and Semiquantitative Signal-based and Signal-independent Analyses

### Apparent T<sub>2</sub>-Relaxation Time (T<sub>2app</sub>)

Tibial nerve T<sub>2app</sub> was lower in RRMS at the thigh (66.1±0.6 ms) and at the lower leg (62.1±0.7 ms) compared to controls (thigh: 69.9±0.6 ms,  $p < 0.0001$ ; lower leg: 67.5±1.0 ms,  $p < 0.0001$ ; Fig. 1a,b). A proximal-to-distal gradient in tibial nerve T<sub>2app</sub> from the thigh to the lower leg was identified in RRMS ( $p < 0.0001$ ) and controls ( $p = 0.0267$ ). Differences between tibial nerve T<sub>2app</sub> at the left versus the right mid to distal thigh were not observed in RRMS (left 65.8±0.7 ms versus right 65.9±0.8 ms,  $p = 0.91$ ) or controls (left 69.2±0.9 ms versus right 69.4±0.8 ms,  $p = 0.92$ ). When separating the RRMS group into patients who were diagnosed less than 3 years ago (RRMS < 3 years) and those diagnosed more than 3 years (RRMS > 3 years) ago, ANOVA revealed group differences at the thigh ( $p < 0.0001$ ,  $F = 10.56$ ) and at the lower leg ( $p < 0.0001$ ,  $F = 10.17$ ). In detail, T<sub>2app</sub> was lower in RRMS > 3 years (thigh: 66.3±0.7 ms,  $p = 0.0004$ ; lower leg: 62.3±0.8 ms,  $p = 0.0003$ ) and in RRMS < 3 years (thigh: 65.6 ms,  $p = 0.0012$ ; lower leg: 61.6 ms,  $p = 0.0029$ ) compared to controls, while differences between RRMS > 3

and RRMS < 3 years did not exist (thigh:  $p = 0.86$ ; lower leg:  $p = 0.91$ ).

Tibial nerve T<sub>2app</sub> at the thigh showed an inverse correlation with RRMS patient age ( $p = 0.0101$ ,  $r = -0.3351$ ) and the EDSS ( $p = 0.0209$ ,  $r = -0.3080$ ), but not with any other demographic, or clinical parameters; however, positive correlations were found between proximal tibial nerve T<sub>2app</sub> and tibial nerve CMAPs ( $p = 0.0142$ ,  $r = 0.3204$ ) and NCVs ( $p = 0.0315$ ,  $r = 0.2827$ ). No further correlations were found between proximal or distal tibial nerve T<sub>2app</sub> and any other demographic, clinical, or electrophysiologic parameters.

### Proton Spin Density (ρ)

Tibial nerve ρ was higher in RRMS patients at the thigh (473.2±12.1 a.u.) and at the lower leg (461.2±11.4 a.u.) compared to controls (thigh: 410.1±6.1 a.u.,  $p < 0.0001$ ; lower leg: 418.0±7.5 a.u.,  $p = 0.0098$ ; Fig. 1c,d). A proximal-to-distal gradient between tibial nerve ρ at thigh and at lower leg level was not present in RRMS ( $p = 0.31$ ) or controls ( $p = 0.43$ ). Likewise, there were no side differences in tibial nerve ρ in RRMS (left 482.0±18.4 a.u. versus right 456.3±10.1 a.u.,  $p = 0.39$ ) or controls (left 412.9±7.1 versus right 413.8±7.0;  $p = 0.99$ ). Group differences were identified between RRMS < 3 years vs. RRMS > 3 years vs. controls at the thigh ( $p < 0.0001$ ,  $F = 11.71$ ) and at the lower leg ( $p = 0.0011$ ,  $F = 7.278$ ). Post hoc analyses identified differences between RRMS > 3 years (thigh: 483.8±14.2 a.u.; lower leg: 473.9±14.0 a.u.) and controls (thigh:  $p < 0.0001$ ; lower leg:  $p = 0.0009$ ), but not between RRMS < 3 years (thigh: 442.8±22.1 a.u.; lower leg: 427.9±16.2 a.u.) and

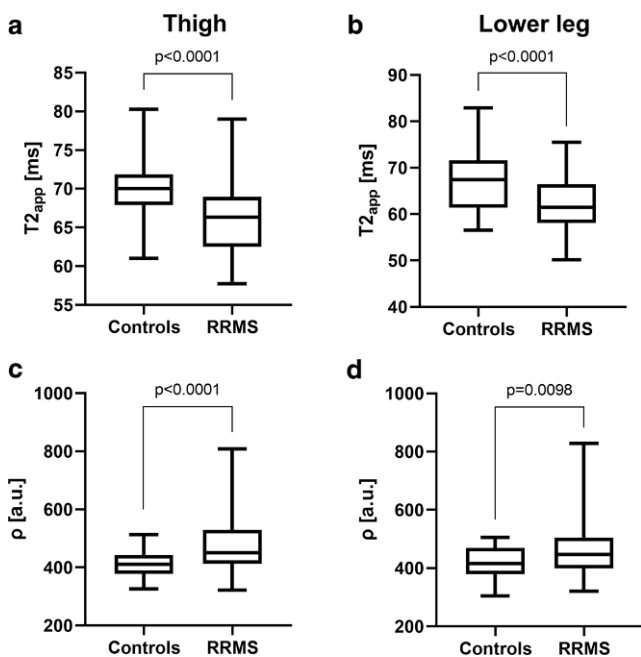


**Fig. 1** Quantitative microstructural MRN markers. Nerve  $T2_{app}$  (a, b) and nerve  $\rho$  (c, d) mean values at the thigh (a, c) and at the lower leg (b, d) were plotted separately for controls and RRMS in a box and whisker plot. Both microstructural markers differentiated well between RRMS patients and healthy controls when measured at the thigh and also at the lower leg. Significant differences are indicated by respective  $p$  values. *a.u.* arbitrary units,  $\rho$  proton spin density, *RRMS* relapsing-remitting multiple sclerosis,  $T2_{app}$  apparent T2-relaxation time

controls (thigh:  $p=0.29$ ; lower leg:  $p=0.88$ ) or between RRMS > 3 years and RRMS < 3 years (thigh:  $p=0.15$ ; lower leg:  $p=0.08$ ).

The  $\rho$  of the tibial nerve at the thigh or at the lower leg did not correlate with any demographic, clinical, or electrophysiologic parameters.

### T2w Signal

Additional evaluations of tibial nerve T2w signal revealed no differences between RRMS and controls at thigh level (RRMS  $132.1 \pm 5.9$  a.u. versus controls  $122.6 \pm 2.9$  a.u.,  $p=0.11$ ; Fig. 2a) or at the lower leg (RRMS  $115.5 \pm 2.8$  a.u. versus controls  $111.3 \pm 2.6$  a.u.,  $p=0.28$ ; Fig. 2b). A proximal-to-distal gradient in tibial nerve T2w signal was detected in RRMS patients ( $p=0.0008$ ), but not in controls ( $p=0.087$ ). Differences in tibial nerve T2 signal between the left and right mid to distal thigh were not detected (RRMS: left  $133.6 \pm 5.8$  a.u. versus right  $129.6 \pm 3.9$  a.u.,  $p=0.76$ ; controls: left  $123.4 \pm 4.5$  a.u. versus right  $120.6 \pm 3.0$  a.u.,  $p=0.74$ ). Upon visual evaluation, nerve lesion distribution in RRMS was disseminated and heterogeneous with slightly hyperintense fascicles being located next to normointense appearing nerve fascicles on nerve cross-sections (Fig. 3).

Tibial nerve T2w signal inversely correlated with male sex (thigh:  $p=0.0005$ ,  $r=-0.4460$ ; lower leg:  $p=0.0012$ ,  $r=-0.4045$ ), and tibial nerve F-waves (thigh:  $p=0.032$ ,  $r=-0.2867$ ; lower leg:  $p=0.0067$ ,  $r=-0.3495$ ), while correlating positively with tibial nerve CMAPs (thigh:  $p=0.0094$ ,  $r=0.3385$ ; lower leg:  $p=0.0128$ ,  $r=0.3169$ ) and NCVs (thigh:  $p=0.0188$ ,  $r=0.3076$ ; lower leg:  $p=0.0039$ ,  $r=0.3647$ ). Tibial nerve T2 signal at the lower leg did not correlate with any demographic, clinical, or electrophysiologic parameters.

### Cross-sectional Area (CSA)

Tibial nerve CSA at the thigh was slightly increased in RRMS ( $17.3 \pm 0.4$  mm<sup>2</sup>) versus controls ( $15.1 \pm 0.3$  mm<sup>2</sup>,  $p<0.0001$ ; Fig. 2c), while no such differences existed at the lower leg (RRMS  $9.1 \pm 0.4$  mm<sup>2</sup> versus controls  $8.5 \pm 0.3$  mm<sup>2</sup>,  $p=0.38$ ; Fig. 2d). As expected and due to the physiologic anatomical course, tibial nerve CSA was higher at the thigh than at the lower leg in RRMS and controls (each  $p<0.0001$ ). Analysis of tibial nerve CSA at mid to distal thigh level revealed no differences between the left and right side (RRMS: left  $66.6 \pm 2.2$  mm<sup>2</sup> versus

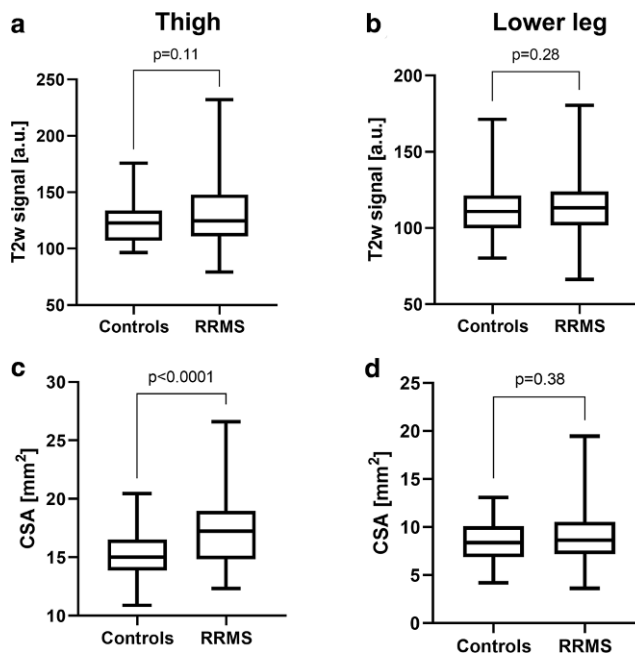


**Fig. 2** Semi-quantitative T2w signal and quantitative morphometric MRN markers. Nerve T2w signal (a, b) and nerve CSA (c, d) mean values at the thigh (a, c) and at the lower leg (b, d) were plotted separately for controls and RRMS in a box and whisker plot. While nerve T2w signal did not separate between RRMS patients and healthy controls, nerve CSA was higher in RRMS than in controls, but only when measured at the thigh and not at the lower leg. Significant differences are indicated by respective  $p$  values. *CSA* cross-sectional area, *RRMS* relapsing-remitting multiple sclerosis



**Fig. 3** MRN source images. Representative magnetic resonance neurography (MRN) images (axial dual-echo turbo spin echo relaxation sequences with spectral fat saturation) at the left proximal thigh (**a, b**), distal thigh (**c, d**), proximal lower leg (**e, f**), and distal lower leg (**g, h**) are shown at equal slice positions in a healthy control (*left*: **a, c, e, g**) and a patient with relapsing-remitting multiple sclerosis (*right*: **b, d, f, h**). Details show the segmented tibial fascicles within the sciatic nerve (**a–d**) and their distal continuation as tibial nerve (**e–h**). Note the diffuse, heterogeneous, and hyperintense lesion distribution in RRMS compared to the control. In RRMS, nerve CSA was also higher at the proximal and distal thigh, but not at the lower leg

right  $65.4 \pm 1.6 \text{ mm}^2$ ,  $p=0.96$ ; controls: left  $58.4 \pm 1.4 \text{ mm}^2$  versus right  $58.8 \pm 1.6 \text{ mm}^2$ ,  $p=0.91$ ).

Tibial nerve CSA at the thigh correlated positively with patient weight ( $p=0.0076$ ,  $r=0.3530$ ), male sex ( $p=0.0151$ ,  $r=0.3234$ ), the EDSS ( $p=0.0418$ ,  $r=0.2781$ ) and disease duration ( $p=0.0168$ ,  $r=0.3183$ ). Inverse correlations were detected between tibial nerve CSA at thigh level and tibial nerve CMAPs ( $p=0.0016$ ,  $r=-0.4125$ ), and sural nerve SNAPs ( $p=0.0173$ ,  $r=-0.3171$ ) and NCVs ( $p=0.0337$ ,  $r=-0.2843$ ). No correlations with any demographic, clinical, or electrophysiologic parameters were found for tibial nerve CSA at the lower leg.

## Discussion

Demyelination in MS is traditionally regarded as an autoimmune disease exclusively affecting the CNS. Even though several histopathologic studies detected areas of additional demyelination in the peripheral nerves of MS patients, these findings were attributed to concomitant neuropathies caused by malnutrition or anemia, rather than to MS itself [10–12, 23, 24]. Electrophysiologic studies were inconclusive and showed an inhomogeneous picture of peripheral nerve electrophysiologic properties in MS [13, 25]. A recent pilot study applying MRN with high structural resolution, conducted by Jende et al., was the first to reliably demonstrate peripheral nerve involvement in an unselected cohort of MS patients by directly visualizing peripheral nerve lesions in vivo [15]. That study was mainly based on the proximal-to-distal assessment of nerve T2w signal at the lower extremities, a MRN parameter that cannot be directly quantified, but can be influenced by external factors, such as field inhomogeneities, radiofrequency excitation field inhomogeneity, nonuniform receiver coil sensitivity, or different signal attenuation for the imaged slabs [16]. Additional morphometric, signal-independent information was provided by measuring proximal-to-distal alterations of nerve CSA; however, a major limitation of the previous study was that more important quantitative microstructural data derived from T2 relaxometry, necessary to understand the pathomorphologic origin behind the occurrence of PNS lesions in MS, was only gathered at a small anatomical section at the distal thigh [15].

Here, we present a comprehensive characterization and quantification of lower extremity peripheral nerve involvement from the proximal thigh to the distal lower leg in a cohort of clinically, and electrophysiologically well-examined patients exclusively with RRMS. Our results show (i) that peripheral nerve lesions in RRMS are characterized by a decrease in  $T2_{\text{app}}$  and an increase in  $\rho$  and CSA, while no differences were observed for T2w signal, and (ii) that the microstructural quantitative MRN marker  $T2_{\text{app}}$  and  $\rho$

are altered at the thigh and the lower leg with proximal predominance.

$T2_{app}$  and  $\rho$  are quantitative MRN markers that provide supplementary information on the integrity and macromolecular composition of nerve tissue by reflecting changes in the biochemical microstructure [26–31]. Initially, both markers were utilized for imaging of the CNS, before they were successfully applied in the PNS [18]. In recent years,  $T2_{app}$  and  $\rho$  were increasingly used to quantify nerve damage in a multitude of different diffuse neuropathies, in which distinct directions of change in  $T2_{app}$  and  $\rho$  (either combined or opposing decrease and/or increase in  $T2_{app}$  and  $\rho$ ) were identified representing the underlying disease entity. In detail, PNPs of different etiology, such as hereditary transthyretin (ATTRv) amyloidosis, systemic light chain amyloidosis, diabetic, and alcoholic neuropathy were characterized by an early increase in  $\rho$ , indicating demyelination, while  $T2_{app}$  was additionally increased in more advanced stages [18–21, 32]. Furthermore,  $\rho$  detected nerve damage in clinically and electrophysiologically completely asymptomatic carriers of the variant transthyretin gene or in alcohol-dependent patients without clinically overt PNP [18, 21, 32]. Nerve damage in the neurodegenerative motor neuron disease, 5q-linked spinal muscular atrophy (SMA), was characterized by an increase in  $T2_{app}$  and a decrease in  $\rho$  [33], which can be explained by the decay of lower motor neurons and the subsequent axonal loss accounting for the predominant pathomorphologic mechanism in SMA. In RRMS, as an example of a demyelinating disease, nerve lesions were characterized by a decrease in  $T2_{app}$  and an increase in  $\rho$ , a unique alteration among the neuropathies investigated with quantitative MRN so far.

Since MRN was first developed three decades ago, an increase in nerve T2w signal has become the most established, yet unspecific MRN criterion to detect nerve damage, especially in traumatic nerve injury or entrapment neuropathies [34–41]. A prolonged  $T2_{app}$ , caused by an increase in the number of free water protons in the extracellular compartment, was suspected as the main factor leading to a T2w signal increase [42–44]; however, in our RRMS cohort, T2w signal along the sciatic and tibial nerves was not significantly altered, yet a multitude of nerve fascicles appeared to be hyperintense upon visual inspection of the acquired T2 relaxometry sequences (Fig. 3). The observed decrease in  $T2_{app}$  might appear contradictory, however, the formula calculating the T2 decay ( $S(TE) = \rho * \exp(-TE / T2_{app})$ ;  $S$  = signal,  $TE$  = echo time) demonstrates that a combined increase in  $T2_{app}$  and  $\rho$ , an increase of one parameter with constancy of the other parameter, or an increase of one parameter outweighing the decrease of the other parameter, can lead to an increased T2w signal. In RRMS, the visually observed T2w hyperintensity in many nerve fascicles was

caused by an increase in  $\rho$  that was more pronounced than the decrease in  $T2_{app}$ .

Our study results confirm the findings of a previously published proof-of-concept study [15] in an entirely new patient cohort of solely RRMS patients and show that peripheral nerve lesions in RRMS are characterized by an increase in  $\rho$  and a decrease in  $T2_{app}$ . Alterations in the two microstructural MRN markers can be similarly observed at proximal (thigh) and distal (lower leg) peripheral nerves; however, a strong proximal-to-distal gradient was detected for  $T2_{app}$  but not for  $\rho$ . This finding, further supported by the visual impression of a diffuse and heterogeneous appearance of nerve lesions, indicates a disseminated, yet proximally predominant distribution of peripheral nerve lesions in RRMS. Importantly, the observed proximal-to-distal distribution pattern supports the hypothesis that peripheral nerve involvement is directly associated with MS and not caused by a neuropathy of different origin. If peripheral nerve lesions were to occur secondary to more proximally located CNS lesions (for example due to Wallerian degeneration), peripheral nerve lesions would appear rather continuous and segmental [45, 46]. Moreover, a previously published study found an inverse correlation between spinal cord and sciatic nerve T2w-hyperintense lesions [15]. A concomitant PNP can also be excluded, as electrophysiologic examination results were in physiologic ranges, and the nerve lesion distribution as detected by MRN would be expected to appear with a proximal-to-distal gradient in  $\rho$  [18–20, 47]. In our RRMS cohort, the increase in  $\rho$  occurring without a gradient along the proximal and distal tibial nerve, may reflect a potential codemyelination of peripheral nerves. Support for this hypothesis comes from a histopathologic CNS study where areas of increased  $\rho$  in the brain and spinal cord of deceased MS patients correlated with areas of demyelination [48]. While it is known that alterations of  $\rho$  are induced by changes in the macromolecular composition of nerve tissue, the factors that directly contribute to a  $\rho$  increase in MS are not fully understood. One possible explanation is a disruption of the endovascular or rather blood nerve barrier caused by inflammatory processes and an impairment of the lipid-rich myelin sheath, subsequently leading to an increased leakage of plasma proteins [49]. As a result, water molecules might increasingly bind to macromolecules, decreasing the amount of free water protons, which in turn would additionally explain the decrease in  $T2_{app}$ . Moreover, the observed decrease in  $T2_{app}$  points against an endoneural edema as an important contributor of peripheral nerve lesions in RRMS. Here, ongoing studies evaluating magnetization transfer contrast imaging might contribute to a better understanding of interactions between free water molecules and protons bound to macromolecules in the future.

Despite the PNS involvement in RRMS, patients in our cohort remained without overt clinical or electrophysiologic signs of a peripheral neuropathy; however, besides  $\rho$ , all analyzed MRN markers correlated with certain electrophysiologic parameters or the EDSS, indicating that MRN findings represent alterations in nerve conductivity on a subclinical level. Moreover, the observed inverse correlation of  $T2_{app}$  and the positive correlation of CSA with the EDSS might reflect a functional impairment of the PNS in MS, potentially contributing to the overall clinical symptom presentation; a hypothesis that might explain the often inexplicable gap between the severity of clinical symptoms and a comparably low burden of CNS lesions [50, 51]. Similar findings have been observed in asymptomatic carriers of the variant transthyretin gene, where MRN preceded the clinical and electrophysiologic disease onset [18, 32]. Even though the pathomechanism leading to the occurrence of PNS lesions in RRMS is unclear, several studies hypothesized that immune cells or antibodies directed against epitopes that are common to the CNS and PNS might play an important role. As an example, connexins as parts of gap junctions between myelinating cells, were assumed to be involved in a combined PNS and CNS demyelination [23, 24, 52]. Other studies focusing on the transition zone between the central and the peripheral myelin of the trigeminal nerve implied that specific proteins, such as connexin 32 and myelin basic protein, are targeted by inflammatory T cells in MS [24, 53].

Our study is limited by its cross-sectional design that does not allow an interpretation regarding the temporal evolution of peripheral nerve lesions in MS. Future studies investigating the PNS in newly diagnosed MS patients or in patients with clinically or radiologically isolated syndromes would be desirable to study early peripheral nerve involvement. Additional histopathologic studies in patients with RRMS would be beneficial to prove or exclude whether alterations in  $T2_{app}$  and  $\rho$  represent subclinical nerve damage. Furthermore, an additional acquisition and analysis of cerebral and spinal MRI in RRMS patients might clarify whether a combined demyelination of the CNS and PNS occurs or PNS lesions precede CNS manifestation. Evaluation of quantitative MRN markers may be difficult to perform in clinical settings as they require a time-consuming manual segmentation; however, identification of peripheral nerve involvement in RRMS seem to be sufficiently possible based on visual inspection by an experienced radiologist [15].

Our study provides first comprehensive data on the in vivo characterization and proximal-to-distal spatial distribution of peripheral nerve involvement in patients with RRMS. Peripheral nerve lesions in RRMS are characterized by a decrease in  $T2_{app}$ , and an increase in  $\rho$ . While significant differences in quantitative markers could be similarly

observed at the thigh and the lower leg, a strong proximal-to-distal gradient was detected for  $T2_{app}$  but not for  $\rho$ , indicating a disseminated, yet proximal predominance of peripheral nerve lesions. These findings may further contribute to the pathophysiologic understanding and relevance of PNS involvement in RRMS.

**Funding** The study was supported in part by the Medical Faculty of the University of Heidelberg (Olympia Morata stipend grant to J.C.H., and Rahel Goetin-Straus stipend grant to O.F.), and the German Research Foundation (SFB 1118 to S.H., SFB 1158 to J.M.E.J. and M.B.).

**Funding** Open Access funding enabled and organized by Projekt DEAL.

**Conflict of interest** A. Viehöver received lecture honoraria from Roche and Merck. R. Diem received grants from the German Research Foundation (FOR 2289), the Hertie Foundation, and the German Ministry of Education and Research. M. Korporeal-Kuhnke reports lecture honoraria from Novartis, BMS and Merck. O. Fösleitner received the Rahel Goetin-Straus stipend grant from the Medical Faculty of the University of Heidelberg. J.M.E. Jende received grants from the German Research Foundation (SFB 1158), and the International Foundation for Research in Paraplegia. S. Heiland received a research grant from the German Research Foundation (SFB 1118). B. Wildemann received grants from the German Ministry of Education and Research, German Research Foundation, Dietmar Hopp Foundation and Klaus Tschira Foundation, grants and personal fees from Merck, Sanofi Genzyme, Novartis, and personal fees from Alexion, Bayer, Biogen, Teva; none related to this work. M. Bendszus reports personal fees from Boehringer Ingelheim, grants and personal fees from Novartis, grants from Siemens, personal fees from Merck, personal fees from Bayer, grants and personal fees from Guerbet, grants from Hopp Foundation, grants from DFG, grants from European Union, grants from Stryker, personal fees from Teva, personal fees from BBraun, personal fees from Vascular Dynamics, personal fees from Grifols, personal fees from Neuroscios. J.C. Hayes received a research grant, personal fees, lecture honoraria and financial support for conference attendance from Alnylam Pharmaceuticals, the Olympia Morata stipend grant from the Medical Faculty of the University of Heidelberg, lecture honoraria and financial support for conference attendance from Pfizer, and advised for Akcea Therapeutics. A.M. Pietsch, M. Weiler, G. Sam and J.M. Hayes declare that they have no competing interests.

**Open Access** This article is licensed under a Creative Commons Attribution 4.0 International License, which permits use, sharing, adaptation, distribution and reproduction in any medium or format, as long as you give appropriate credit to the original author(s) and the source, provide a link to the Creative Commons licence, and indicate if changes were made. The images or other third party material in this article are included in the article's Creative Commons licence, unless indicated otherwise in a credit line to the material. If material is not included in the article's Creative Commons licence and your intended use is not permitted by statutory regulation or exceeds the permitted use, you will need to obtain permission directly from the copyright holder. To view a copy of this licence, visit <http://creativecommons.org/licenses/by/4.0/>.

## References

- Hoffmann S, Vitzthum K, Mache S, Spallek M, Quarcoo D, Groneberg DA, Uibel S. Multiple Sklerose: Epidemiologie, Pathophysiologie, Diagnostik und Therapie. *Prakt Arb Med.* 2009;17:12–8.



2. Weinshenker BG. The natural history of multiple sclerosis: update 1998. *Semin Neurol.* 1998;18:301–7.
3. Wikström J, Poser S, Ritter G. Optic neuritis as an initial symptom in multiple sclerosis. *Acta Neuro Scandinaica.* 1980;61:178–85.
4. Fletcher SG, Castro-Borrero W, Remington G, Treadaway K, Lemack GE, Frohman EM. Sexual dysfunction in patients with multiple sclerosis: a multidisciplinary approach to evaluation and management. *Nat Clin Pract Urol.* 2009;6:96–107.
5. Fischer M, Kunkel A, Bublak P, Faiss JH, Hoffmann F, Sailer M, Schwab M, Zettl UK, Köhler W. How reliable is the classification of cognitive impairment across different criteria in early and late stages of multiple sclerosis? *J Neurol Sci.* 2014;343:91–9.
6. Faiss JH, Dähne D, Baum K, Deppe R, Hoffmann F, Köhler W, Kunkel A, Lux A, Matzke M, Penner IK, Sailer M, Zettl UK. Reduced magnetisation transfer ratio in cognitively impaired patients at the very early stage of multiple sclerosis: a prospective, multicenter, cross-sectional study. *BMJ Open.* 2014;4:e004409.
7. Weinshenker BG, Bass B, Rice GP, Noseworthy J, Carriere W, Baskerville J, Ebers GC. The natural history of multiple sclerosis: a geographically based study. 2. Predictive value of the early clinical course. *Brain.* 1989;112:1419–28.
8. Lublin FD, Reingold SC, Cohen JA, Cutter GR, Sørensen PS, Thompson AJ, Wolinsky JS, Balcer LJ, Banwell B, Barkhof F, Bebo B Jr, Calabresi PA, Clanet M, Comi G, Fox RJ, Freedman MS, Goodman AD, Inglesse M, Kappos L, Kieser BC, Lincoln JA, Lubetzki C, Miller AE, Montalban X, O'Connor PW, Petkau J, Pozzilli C, Rudick RA, Sormani MP, Stüve O, Waubant E, Polman CH. Defining the clinical course of multiple sclerosis: the 2013 revisions. *Neurology.* 2014;83:278–86.
9. Thompson AJ, Banwell BL, Barkhof F, Carroll WM, Coetzee T, Comi G, Correale J, Fazekas F, Filippi M, Freedman MS, Fujihara K, Galetta SL, Hartung HP, Kappos L, Lublin FD, Marrie RA, Miller AE, Miller DH, Montalban X, Mowry EM, Sorensen PS, Tintoré M, Traboulsee AL, Trojano M, Uitdehaag BMJ, Vukusic S, Waubant E, Weinshenker BG, Reingold SC, Cohen JA. Diagnosis of multiple sclerosis: 2017 revisions of the McDonald criteria. *Lancet Neurol.* 2018;17:162–73.
10. Hasson J, Terry RD, Zimmerman HM. Peripheral neuropathy in multiple sclerosis. *Neurology.* 1958;8:503–10.
11. Schoene WC, Carpenter S, Behan PO, Geschwind N. 'Onion bulb' formations in the central and peripheral nervous system in association with multiple sclerosis and hypertrophic polyneuropathy. *Brain.* 1977;100:755–73.
12. Pollock M, Calder C, Allpress S. Peripheral nerve abnormality in multiple sclerosis. *Ann Neurol.* 1977;2:41–8.
13. Anlar O, Tombul T, Kisli M. Peripheral sensory and motor abnormalities in patients with multiple sclerosis. *Electromyogr Clin Neurophysiol.* 2003;43:349–51.
14. Vogt J, Paul F, Aktas O, Müller-Wiensch K, Dörr J, Dörr S, Bharathi BS, Glumm R, Schmitz C, Steinbusch H, Raine CS, Tsokos M, Nitsch R, Zipp F. Lower motor neuron loss in multiple sclerosis and experimental autoimmune encephalomyelitis. *Ann Neurol.* 2009;66:310–22.
15. Jende JME, Hauck GH, Diem R, Weiler M, Heiland S, Wildemann B, Korporal-Kuhnke M, Wick W, Hayes JM, Pfaff J, Pham M, Bendszus M, Kollmer J. Peripheral nerve involvement in multiple sclerosis: Demonstration by magnetic resonance neurography. *Ann Neurol.* 2017;82:676–85.
16. Milford D, Rosbach N, Bendszus M, Heiland S. Mono-exponential fitting in T2-relaxometry: relevance of offset and first echo. *PLoS One.* 2015;10:e0145255.
17. Jenkinson M, Beckmann CF, Behrens TE, Woolrich MW, Smith SM. FSL. *Neuroimage.* 2012;62:782–90.
18. Kollmer J, Hund E, Hornung B, Hegenbart U, Schönland SO, Kimmich C, Kristen AV, Purrucker J, Röcken C, Heiland S, Bendszus M, Pham M. In vivo detection of nerve injury in familial amyloid polyneuropathy by magnetic resonance neurography. *Brain.* 2015;138:549–62.
19. Kollmer J, Weiler M, Purrucker J, Heiland S, Schönland SO, Hund E, Kimmich C, Hayes JM, Hilgenfeld T, Pham M, Bendszus M, Hegenbart U. MR neurography biomarkers to characterize peripheral neuropathy in AL amyloidosis. *Neurology.* 2018;91:e625–34.
20. Pham M, Oikonomou D, Hornung B, Weiler M, Heiland S, Bäumer P, Kollmer J, Nawroth PP, Bendszus M. Magnetic resonance neurography detects diabetic neuropathy early and with proximal predominance. *Ann Neurol.* 2015;78:939–48.
21. Rother C, Bumb JM, Weiler M, Brault A, Sam G, Hayes JM, Pietsch A, Karimian-Jazi K, Jende JME, Heiland S, Kiefer F, Bendszus M, Kollmer J. Characterization and quantification of alcohol-related polyneuropathy by magnetic resonance neurography. *Eur J Neurol.* 2022;29:573–82.
22. Poncelet A, Weiler M, Hegenbart U, Sam G, Schönland S, Purrucker JC, Hayes JM, Hund E, Bendszus M, Heiland S, Kollmer J. Dual-echo turbo spin echo and 12-echo multi spin echo sequences as equivalent techniques for obtaining T2-relaxometry data: application in symptomatic and asymptomatic hereditary transthyretin amyloidosis as a surrogate disease. *Invest Radiol.* 2022;57:301–7.
23. Gartzon K, Katzarava Z, Diener HC, Putzki N. Peripheral nervous system involvement in multiple sclerosis. *Eur J Neurol.* 2011;18:789–91.
24. Rovira A. Peripheral nervous system involvement in multiple sclerosis. *Mult Scler.* 2017;23:751.
25. Misawa S, Kuwabara S, Mori M, Hayakawa S, Sawai S, Hattori T. Peripheral nerve demyelination in multiple sclerosis. *Clin Neurophysiol.* 2008;119:1829–33.
26. Nitz WR. MR imaging: acronyms and clinical applications. *Eur Radiol.* 1999;9:979–97.
27. Heiland S, Sartor K, Martin E, Bardenheuer HJ, Plaschke K. In vivo monitoring of age-related changes in rat brain using quantitative diffusion magnetic resonance imaging and magnetic resonance relaxometry. *Neurosci Lett.* 2002;334:157–60.
28. Kurki T, Komu M. Spin-lattice relaxation and magnetization transfer in intracranial tumors in vivo: effects of Gd-DTPA on relaxation parameters. *Magn Reson Imaging.* 1995;13:379–85.
29. Miot E, Hoffschir D, Alapetite C, Gaboriaud G, Pontvert D, Fétissou F, Le Pape A, Akoka S. Experimental MR study of cerebral radiation injury: quantitative T2 changes over time and histopathologic correlation. *AJNR Am J Neuroradiol.* 1995;16:79–85.
30. Walimuni IS, Hasan KM. Atlas-based investigation of human brain tissue microstructural spatial heterogeneity and interplay between transverse relaxation time and radial diffusivity. *Neuroimage.* 2011;57:1402–10.
31. Hattingen E, Jurcoane A, Nelles M, Müller A, Nöth U, Mädler B, Mürtz P, Deichmann R, Schild HH. Quantitative MR imaging of brain tissue and brain pathologies. *Clin Neuroradiol.* 2015;25 Suppl 2:219–24.
32. Kollmer J, Sahn F, Hegenbart U, Purrucker JC, Kimmich C, Schönland SO, Hund E, Heiland S, Hayes JM, Kristen AV, Röcken C, Pham M, Bendszus M, Weiler M. Sural nerve injury in familial amyloid polyneuropathy: MR neurography vs clinicopathologic tools. *Neurology.* 2017;89:475–84.
33. Kollmer J, Hilgenfeld T, Ziegler A, Saffari A, Sam G, Hayes JM, Pietsch A, Jost M, Heiland S, Bendszus M, Wick W, Weiler M. Quantitative MR neurography biomarkers in 5q-linked spinal muscular atrophy. *Neurology.* 2019;93:e653–64.
34. Bendszus M, Stoll G. Technology insight: visualizing peripheral nerve injury using MRI. *Nat Clin Pract Neurol.* 2005;1:45–53.
35. Koltzenburg M, Bendszus M. Imaging of peripheral nerve lesions. *Curr Opin Neurol.* 2004;17:621–6.
36. Jarvik JG, Yuen E, Haynor DR, Bradley CM, Fulton-Kehoe D, Smith-Weller T, Wu R, Kliot M, Kraft G, Wang L, Erlich V, Heagerty PJ, Franklin GM. MR nerve imaging in a prospective cohort

- of patients with suspected carpal tunnel syndrome. *Neurology*. 2002;58:1597–602.
37. Kollmer J, Bäumer P, Milford D, Dombert T, Staub F, Bendszus M, Pham M. T2-signal of ulnar nerve branches at the wrist in guyon's canal syndrome. *PLoS One*. 2012;7:e47295.
  38. Filler AG, Kliot M, Howe FA, Hayes CE, Saunders DE, Goodkin R, Bell BA, Winn HR, Griffiths JR, Tsuruda JS. Application of magnetic resonance neurography in the evaluation of patients with peripheral nerve pathology. *J Neurosurg*. 1996;85:299–309.
  39. Kuntz C 4th, Blake L, Britz G, Filler A, Hayes CE, Goodkin R, Tsuruda J, Maravilla K, Kliot M. Magnetic resonance neurography of peripheral nerve lesions in the lower extremity. *Neurosurgery*. 1996;39:750–6; discussion 756–7.
  40. Sollmann N, Weidlich D, Cervantes B, Klupp E, Ganter C, Kooijman H, Rummeny EJ, Zimmer C, Kirschke JS, Karampinos DC. High isotropic resolution T2 mapping of the lumbosacral plexus with T2-prepared 3D turbo spin echo. *Clin Neuroradiol*. 2019;29:223–30.
  41. Kollmer J, Bendszus M, Pham M. MR neurography: diagnostic imaging in the PNS. *Clin Neuroradiol*. 2015;25 Suppl 2:283–9.
  42. Does MD, Snyder RE. Multiexponential T2 relaxation in degenerating peripheral nerve. *Magn Reson Med*. 1996;35:207–13.
  43. Titelbaum DS, Frazier JL, Grossman RI, Joseph PM, Yu LT, Kassab EA, Hickey WF, LaRossa D, Brown MJ. Wallerian degeneration and inflammation in rat peripheral nerve detected by in vivo MR imaging. *AJNR Am J Neuroradiol*. 1989;10:741–6.
  44. Cudlip SA, Howe FA, Griffiths JR, Bell BA. Magnetic resonance neurography of peripheral nerve following experimental crush injury, and correlation with functional deficit. *J Neurosurg*. 2002;96:755–9.
  45. Bendszus M, Wessig C, Solymosi L, Reiners K, Koltzenburg M. MRI of peripheral nerve degeneration and regeneration: correlation with electrophysiology and histology. *Exp Neurol*. 2004;188:171–7.
  46. Hilgenfeld T, Jende J, Schwarz D, Bäumer P, Kollmer J, Heiland S, Bendszus M, Pham M. Somatotopic fascicular lesions of the brachial plexus demonstrated by high-resolution magnetic resonance neurography. *Invest Radiol*. 2017;52:741–6.
  47. Frosch M, Kremers N, Lisko K, Urbach H, Prinz M, Taschner CA. Freiburg Neuropathology Case Conference: a 42-year-old patient with progressive neurological deficits, multiple brain lesions and accompanying affection of peripheral nerves. *Clin Neuroradiol*. 2021;31:529–35.
  48. Nijeholt GJ, Bergers E, Kamphorst W, Bot J, Nicolay K, Castelijns JA, van Waesberghe JH, Ravid R, Polman CH, Barkhof F. Post-mortem high-resolution MRI of the spinal cord in multiple sclerosis: a correlative study with conventional MRI, histopathology and clinical phenotype. *Brain*. 2001;124:154–66.
  49. Davies GR, Ramani A, Dalton CM, Tozer DJ, Wheeler-Kingshott CA, Barker GJ, Thompson AJ, Miller DH, Tofts PS. Preliminary magnetic resonance study of the macromolecular proton fraction in white matter: a potential marker of myelin? *Mult Scler*. 2003;9:246–9.
  50. Rovaris M, Bozzali M, Santuccio G, Ghezzi A, Caputo D, Montanari E, Bertolotto A, Bergamaschi R, Capra R, Mancardi G, Martinelli V, Comi G, Filippi M. In vivo assessment of the brain and cervical cord pathology of patients with primary progressive multiple sclerosis. *Brain*. 2001;124:2540–9.
  51. Miller DH, Grossman RI, Reingold SC, McFarland HF. The role of magnetic resonance techniques in understanding and managing multiple sclerosis. *Brain*. 1998;121:3–24.
  52. Shor N, Amador MD, Dormont D, Lubetzki C, Bertrand A. Involvement of peripheral III nerve in multiple sclerosis patient: report of a new case and discussion of the underlying mechanism. *Mult Scler*. 2017;23:748–50.
  53. Pichiecchio A, Bergamaschi R, Tavazzi E, Romani A, Todeschini A, Bastianello S. Bilateral trigeminal enhancement on magnetic resonance imaging in a patient with multiple sclerosis and trigeminal neuralgia. *Mult Scler*. 2007;13:814–6.